Functionalization of synthetic talc-like phyllosilicates by alkoxyorganosilane grafting

Karine Joncoux-Chabrol, Marie Gressier, Nadine Pébère, Marie-Joëlle Menu, François Martin, Jean-Pierre Bonino, Claire Marichal, Jocelyne Brendlé

Karine Chabrol,[ab] Marie Gressier,*[a] Nadine Pebere,[b] Marie-Joëlle Menu,[a] François Martin,[c] Jean-Pierre Bonino,[a] Claire Marichal[d] and Jocelyne Brendle[d]

DOI: 10.1039/c0jm01276a

A range of talc-like phyllosilicates were prepared *via* a hydrothermal synthesis performed at five different temperatures from 160 to 350 °C. The organization of the lattice and the degree of crystallinity of the new materials were evaluated by different techniques such as XRD, FTIR, solid-state ^{29}Si NMR, TEM, FEG-SEM and TG-DTA. When synthesized at low temperature the material presents high degree of hydration, low crystallinity and flawed structure. This was attributed to stevensite-talc interstratified product present in the samples. The stevensite/talc ratio and the hydration decrease in the talc-like phyllosilicate samples when the hydrothermal synthesis temperature increases and so the crystallinity becomes higher. A thermal treatment at 500 °C allowed a significant flaw reduction in talc-like phyllosilicate structure; the synthesized sample at 350 °C and heat treated presents a structure close to that of talc. The different talc-like phyllosilicates were grafted covalently by two organoalkoxysilane reagents, N-(3-triethoxysilylpropyl)-4,5-dihydroimidazole (IM2H) and 2-hydroxy-4-(3-triethoxysilylpropoxy)-diphenylketone (HTDK). The grafted amounts of the hybrids, determined by elemental analysis and confirmed by thermogravimetric data, are dependent on the hydrothermal synthesis temperature and organoalkoxysilanes; they become smaller when the synthesis temperature increases and when HTDK is used. FTIR and solid-state ^{13}C CP MAS NMR were applied to characterize the grafted organic groups. So, in this work it is shown that by choosing the hydrothermal synthesis temperature or by performing an additional annealing it is possible to adjust the amount of defects in the structure of talc-like phyllosilicates which seems to be strongly correlated to the grafting performance.

1. Introduction

Today synthesis of organic–inorganic hybrid materials is not only a challenge for academic research with the goal to conceive new materials, but their improved or unusual characteristics open a land of promising applications in many fields such as optics, electronics, mechanics, energy, biology, medicine.[1,2] The growing interest for creating such materials and devices results from the fact that they combine the best of the inorganic and organic world. Recently, organic–inorganic hybrids of class II (classification of Sanchez and Ribot), have been actively studied.[2] They are particularly interesting because they present strong-type interactions between the inorganic and organic components. This strong link enables a durable immobilization of the organic groups on the inorganic surface, and therefore it avoids their leaching when the hybrids are used in solution.

Concerning the inorganic clay framework, talc is particularly interesting owing to its mechanical and lubricant properties which could also be used to develop new low friction composite materials.[3,4] Talc is currently used as filler, coating or dusting agent in paints, lubricants, plastics, cosmetics, pharmaceuticals and ceramics. It is a layered magnesium silicate mineral with the formula $Si_4Mg_3O_{10}(OH)_2$. The ideal talc lamellar structure, described by several authors, is composed of superposed elementary sheets stacked on top of one another.[5–8] Each of them is constituted by a layer of magnesium-oxygen/hydroxyl octahedra sandwiched between two layers of silicon-oxygen tetrahedra. In these sheets, the atoms are linked by covalent bonds whereas the sheets are bonded together only by weak van der Waals interactions and hence talc readily undergoes cleavage to form lamellar shaped particles. The basal faces of the layers, which account for 90% of the total surface,[9] do not contain hydroxyl groups or active ions and the edge faces contain only a few –SiOH and –MgOH groups. Therefore, talc is characteristically hydrophobic and inert. Natural talcs have chemical compositions close to the ideal one (*i.e.* $Mg_3Si_4O_{10}(OH)_2$), however according to their origin, the different talc varieties can contain quantities of iron, or small quantities of aluminium and fluorine or traces of manganese, titanium, chromium, nickel, calcium, sodium and potassium.[10–13] Sometimes magnesium and silicon atoms can be replaced by other elements in the octahedral

[a]*Université de Toulouse, Institut Carnot CIRIMAT, UMR 5085 UPS/INPT/CNRS, Université Paul Sabatier, 118 route de Narbonne, 31062 Toulouse cedex 9, France. E-mail: gressier@chimie.ups-tlse.fr; Fax: (+33)561556163; Tel: (+33)561556120*

[b]*Université de Toulouse, Institut Carnot CIRIMAT, UMR 5085 UPS/INPT/CNRS, ENSIACET, 4 allée Emile Monso, BP 44362, 31432 Toulouse cedex 4, France*

[c]*Laboratoire des Mécanismes et Transferts en Géologie, UMR 5563 UR 154 CNRS, Université Paul Sabatier IRD Observatoire Midi-Pyrénées, 14 avenue Edouard Belin, 31400 Toulouse, France*

[d]*Equipe Matériaux à Porosité Contrôlée, Institut de Science des Matériaux de Mulhouse, LRC CNRS 7228, Université de Haute Alsace, 3, rue A. Werner, 68093 Mulhouse, France*

and tetrahedral sites and some other times the talc can be associated with another material such as chlorite. The advantage of synthetic minerals over the natural one is due to the possibility to obtain samples with well-defined chemical composition, high purity, homogeneous and controlled porosity. For instance, these properties are needed for catalytic processes and it was shown that catalyst systems constituted of talc-based hybrids are better catalysts for alkanes and alkenes oxidations than the molecular catalyst.[14] In these catalytic systems talc is the support for iron porphyrin catalysts through covalent binding. Covalently linked inorganic–organic lamellar hybrids can be obtained by two methods: one step sol–gel synthesis[15–20] or grafting of inorganic framework by organic molecules.[21,22] In the first method, several reports have shown how to prepare at room temperature covalently linked inorganic–organic lamellar nanocomposites based on the talc structure. These materials have been obtained through the procedure of organoalkoxysilanes copolymerization with magnesium salts. By this preparative method, organic moieties are covalently bonded to the inorganic framework but the presence of high amounts of organic matter leads usually to solids having low crystallinity. In the second method, the rare silanol functions located at the surface of talc are able to form covalent bonds with suitable chemical groups such as anhydride or alkoxysilane functions. Organo-grafted talc derivatives were obtained by using the coupling agents 3-aminopropyl-, N-propylethylenediamine and N-propyltriethylenediaminetrimethoxysilane in anhydrous conditions.[21] This grafting reaction does not modify the original structure of the inorganic support and organic groups are supported on basal surface of the particles. This phenomenon can be explained by the difficult exfoliation of talc due to high energy between the sheets of natural talc.[23] However, the coating of particles surface with organic groups modifies the surface properties of solids and these reactions can be controlled for specific applications.[14]

The goal of the present investigation was to obtain covalently grafted hybrids based on talc with varied and controlled grafting ratios. However talc is known for its limited chemical reactivity so the preparation of a range of synthetic talc-like phyllosilicates with different ability to react was investigated. Indeed, the preparation of synthetic talc-like phyllosilicates was the object of studies for several years and it ended recently giving satisfactory results in particular compatible with the obligations of quality and operating cost at the industrial scale.[24–26] The control of the synthesis parameters could permit the control of the hydration degree and thus to act on the inertia/reactivity balance, allowing the grafting by covalent bonding of organic groups on the hydroxyl groups of synthetic talc-like phyllosilicates. Another important feature of this synthesis is the possibility to access nanometric sized particles.

In this paper we describe first the synthesis and physicochemical characterization of a range of talc-like phyllosilicates hydrothermally synthesized at different temperatures. The synthesis consists of hydrothermal treatment of magnesium chloride and sodium metasilicate with a Si/Mg molar ratio equal to 4/3.[26] The process is based on a preliminary work which described a synthesis leading to the formation of stevensite, kerolites and/or talc according to the operating conditions.[27] In our work we investigated the effects of the hydrothermal synthesis temperature and a heat treatment on the composition

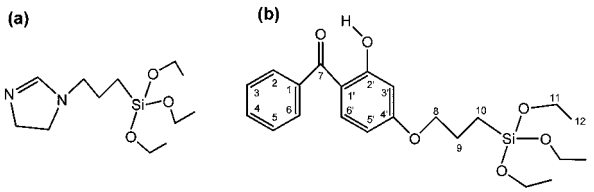

Scheme 1 Structure of IM2H **(a)** and HTDK **(b)**.

of the talc-like phyllosilicate obtained; the products are designated Tx (x = 160, 200, 240, 300 and 350 related to their hydrothermal synthesis temperature) and TTx when the sample underwent a supplementary heat treatment at 550 °C. Secondly we report their functionalization *via* a grafting reaction in toluene using N-(3-triethoxysilylpropyl)-4,5-dihydroimidazole (IM2H) and 2-hydroxy-4-(3-triethoxysilylpropoxy)-diphenylketone (HTDK) as silylating agents (Scheme 1).

The steric hindrance of these molecules is not particularly favourable to the grafting, so they present a good means of evaluating the grafting ability of Tx and TTx samples. The obtained nanohybrids are designated Tx-A, TTx-A and Tx-B, TTx-B when IM2H and HTDK were used, respectively. The grafting reaction was done in toluene medium in order to minimize the hydrolysis and polymerization of organoalkoxysilanes and therefore favour the grafting reaction.[28,29] The organization of the lattice and the degree of crystallinity of these new materials were evaluated by different techniques such as XRD, FTIR, ^{29}Si CP MAS and MAS NMR, TEM, FEG-SEM and TG-DTA. The amount of grafted organosilane was determined by elemental analysis and confirmed by thermogravimetric data. FTIR and ^{13}C CP MAS NMR were applied to characterize the grafted organic groups.

2. Experimental section

2.1. Materials

Hexahydrated magnesium chloride ($MgCl_2 \cdot 6H_2O$), pentahydrated sodium metasilicate ($Na_2SiO_3 \cdot 5H_2O$), strontium chloride ($SrCl_2$) and hydrochloric acid were purchased from Aldrich. The silylating agents N-(3-triethoxysilylpropyl)-4,5-dihydroimidazole (IM2H) and 2-hydroxy-4-(3-triethoxysilylpropoxy)-diphenylketone (HTDK) were obtained from ABCR. The reagents were used without purification. A sample of natural talc, from the Trimouns deposit located in the French Pyrénées, was used for comparison with synthesized talc-like phyllosilicates. Its composition is: $[Mg_{2.978}Fe^{2+}_{0.019}Mn^{2+}_{0.001}Fe^{3+}_{0.005}Al_{0.007}]_{\Sigma 3}$ $[Si_{3.984}Fe^{3+}_{0.004}Al_{0.007}]_{\Sigma 4}O_{10}(OH)_{1.952}F_{0.048}$.[11] Toluene and acetone were purified by distillation in an inert atmosphere before use.

2.2. Characterization

X-Ray powder diffraction patterns were obtained using a INEL CPS 120 powder diffractometer (Ni-filtered Co–Kα radiation, $\lambda = 0.178897$ nm), between 0.293 and 107.274° 2θ with a step size of 0.029°.

Fourier transform infrared (FTIR) spectra were recorded using a Nicolet Nexus FTIR spectrometer on powder-pressed KBr pellets. Diffuse reflectance infrared spectra (DRIFT) were

obtained with a Perkin-Elmer 1760 X spectrometer and a DTGS detector.

Elemental analyses of Na, Si, Mg and Sr (if necessary) were performed by X-Ray Fluorescence (XRF) with a Magix Philips (2.4 KW). The synthesized materials were either pressed into pellets or calcined and mixed with lithium tetraborate before being fused to form beads.

^{1}H decoupled ^{29}Si MAS (Magic Angle Spinning) Nuclear Magnetic Resonance (NMR) spectra were recorded on a Bruker Avance II 400 spectrometer (B0 = 9.4T). Samples were packed in a 7 mm diameter cylindrical zirconia rotor and spun at a spinning frequency of 4 kHz. A $\pi/6$ pulse duration of 2.6 μs with a recycle delay of 80 s was used. ^{1}H–^{29}Si and ^{1}H–^{13}C CP MAS NMR experiments were also performed in natural abundance at frequencies of 79.393 and 100.484 MHz for carbon and silicon, respectively. These experiments were recorded with a proton $\pi/2$ pulse duration of 3 μs, a contact time of 3 ms (for ^{29}Si) and 2 ms (for ^{13}C) and a recycle delay of 5 s. ^{1}H, ^{29}Si and ^{13}C chemical shifts are relative to tetramethylsilane (TMS).

Decompositions of the NMR spectra to extract the proportion of the corresponding species were performed with the DMfit software.[30]

The nitrogen adsorption-desorption isotherms were determined at 77 K, using a volumetric method, with a Micrometrics TriStar II 3020 apparatus. The isotherms were recorded in the 0.008–0.994 relative pressure range. Nitrogen of high purity (99.999%) was used. Samples were outgassed for 10 h at 90 °C under vacuum before analysis.

The amount of grafted organosilane on each sample was determined by elemental analysis of C, H and N performed on a Carlo Erba Thermoquest Elementary Analyser (EA 1110).

Thermogravimetric (TG) and differential thermal (DT) analyses were carried out on a Setaram TG-DTA 92 thermobalance using 20 mg of sample; α-alumina was used as a reference. The heating rate was 5 °C min^{-1}, the temperature range was 20 to 1200 °C, and the analyses were done using a 1.5 L h^{-1} air flow.

Transmission electron microscopy (TEM) investigations were carried out on a JEOL 2010 microscope operating at 200 kV. Prior to observation, the powders were dispersed in ethanol and a droplet was deposited onto a carbon-coated copper grid and left to dry in air at room temperature. Scanning electron microscopy (FEG-SEM) analyses were done on a JEOL JSM 6700 F microscope operating at 3 kV.

2.3. Synthesis of talc-like phyllosilicates and thermal treatment

Talc-like phyllosilicates were synthesized according to a hydrothermal process rather similar to that indicated by Martin *et al.*[26] A mixture of aqueous solution of hexahydrated magnesium chloride (0.075 mole in 50 cm^3 of water) and 50 cm^3 hydrochloric acid (1 mol dm^{-3}) was added to an aqueous solution of pentahydrated sodium metasilicate (0.1 mol in 250 cm^3 of water), leading to a Si/Mg molar ratio equal to 4/3. Immediately an amorphous product was formed and it was collected by centrifugation (7000 rpm for 15 min). The obtained solid was washed with water, centrifuged (7000 rpm for 15 min) twice to remove sodium and chloride ions, and a white compound named precursor was collected. The talc-like phyllosilicate was obtained by hydrothermal treatment of the precursor (100 g) in a Teflon-lined autoclave for 48 h under autogeneous pressure. The hydrothermal synthesis was performed at 5 different temperatures: 160, 200, 240, 300 and 350 °C. The autoclave was cooled to room temperature and the sample was collected. Afterwards the product was dried during 24 h at 120 °C and milled, resulting in about 20 g of Tx talc-like phyllosilicate with x representing the value of the hydrothermal synthesis temperature. After synthesis, part of sample T160 (1 g) was mixed with 25 cm^3 of a 0.10 mol dm^{-3} aqueous solution of strontium chloride and stirred at room temperature during 2 h. The procedure was repeated twice. Sample was then recovered by filtration and thoroughly washed with distilled water before being dried at 60 °C overnight.

In order to observe the influence of a thermal treatment on the obtained Tx talc-like phyllosilicates, a sample of each material was heated at 550 °C during 4 h resulting in TTx talc-like phyllosilicates.

2.4. Grafting step

The organotriethoxysilane N-(3-triethoxysilylpropyl)-4,5-dihydroimidazole (IM2H) or 2-hydroxy-4-(3-triethoxysilylpropoxy)-diphenylketone (HTDK) (14 mmol) was added to a stirred solution of talc-like phyllosilicate (1.5 g) in dry toluene (50 cm^3) at 110 °C under nitrogen atmosphere. The reaction mixture was left stirring for 48 h under these conditions. At the end of the reaction the sample was centrifuged at 3000 rpm for 12 min. The clear supernatant was decanted from the solid deposit composed of the functionalized phyllosilicate. The solid was washed and centrifuged (3000 rpm for 12 min) three times with acetone and finally dried under vacuum for 2 h resulting in Tx-A, TTx-A and Tx-B when IM2H and HTDK were used, respectively.

3. Results and discussion

3.1. Tx talc-like phyllosilicates characterization

The X-ray powder diffraction patterns of the precursor, Tx talc-like phyllosilicates and natural talc with the peak

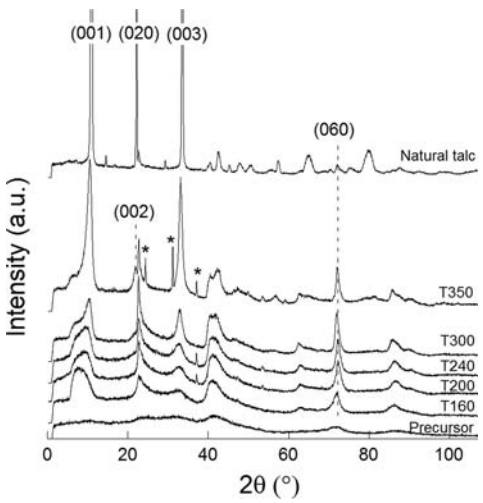

Fig. 1 X-Ray powder diffraction patterns of the precursor, Tx talc-like phyllosilicates and natural talc (* NaCl); a.u.: arbitrary unit.

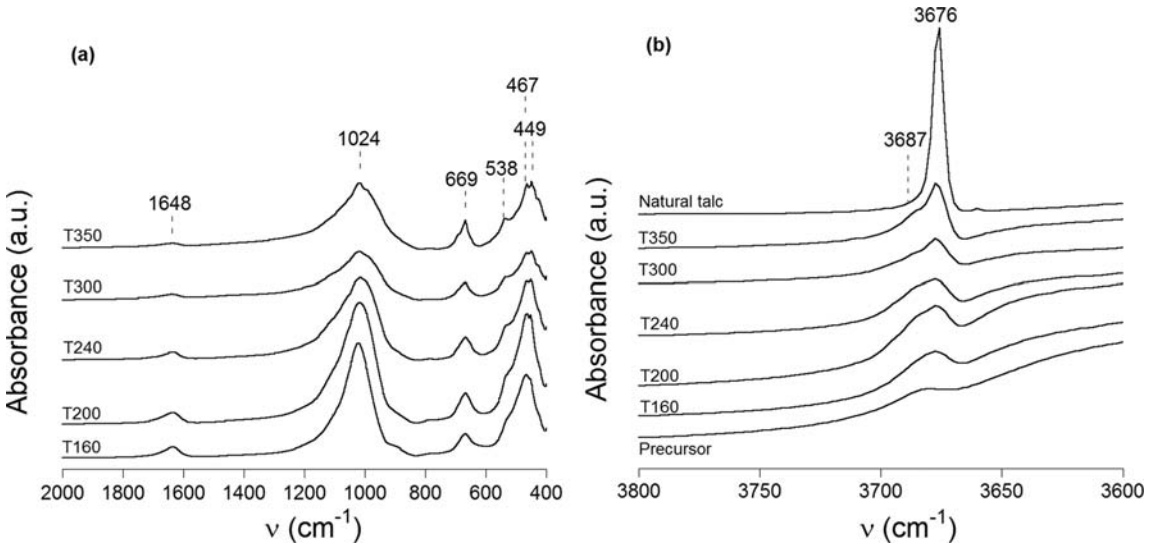

Fig. 2 FTIR spectra of Tx talc-like phyllosilicates in the 2000–400 cm^{-1} **(a)** and enlargement in the 3800–3600 cm^{-1} frequency range **(b)**; a.u.: arbitrary unit.

assignments are shown in Fig. 1. Each sample showed d interreticular distances characteristic values for (001), (020), (003) and (060) reflections of talc structure.[11,31,32] The (060) reflection was observed at 0.151 and 0.152 nm for T160 and T350, respectively; these values are characteristic of a trioctahedral 2 : 1 phyllosilicate structure (in the octahedral sheets each O atom or OH group is surrounded by three divalent cations).[33–35]

The X-ray powder diffraction patterns of T350 sample showed three sharp peaks (0.423, 0.333 and 0.280 nm) assigned to NaCl precipitated during the synthesis of the precursor which was not washed enough for this sample. The characteristic (002) reflection of talc structure appeared clearly in the T350 diffractogram. This indicated that a hydrothermal synthesis temperature of 350 °C led to a mineral with characteristics closer to those of talc. The T160, T200, T240 and T300 samples presented relatively broad (00l) reflections, indicating a low degree of crystalline coherence along the stacking axis. For clay minerals having a low crystallinity along the z axis, the apparent basal spacing $d_{(001)}$, taken directly from the broad (001) diffraction peak, is quite different from the real one, in this case the true $d_{(001)}$ value can be obtained from $d_{(003)}$.[27] The basal $d_{(001)}$ were thus calculated from (003) diffraction peak, the values were 0.945 and 0.941 nm for T160 and T350, respectively, due to stacking faults in 001 direction and small numbers of layers along z axis. These values are slightly higher compared to the talc parent structure ($d_{(001)} = 0.934$ nm).[36] The temperature of hydrothermal synthesis influenced considerably the crystallinity of the materials since the biggest peaks intensity and the reduction of the full width at half height with the increase of the synthesis temperature proved the best crystallinity. This fact was clearly illustrated by the intensity and the shape of (001) reflection; indeed the powder diffraction patterns for low hydrothermal synthesis temperatures presented a broad peak whereas T350 sample exhibited a sharp peak clearly separated from another less intense peak at smaller diffraction angles. The position, the shape and the intensity of the (001) reflection for T160 indicated clearly that this material consisted of random stevensite-talc mixed-layered phases with a high percentage of stevensite.[27] Indeed stevensite is a magnesium silicate which has the same chemical composition as talc but unlike this latter, magnesium cations are present both in the interlayer space and in the octahedral sheet.[37] A defect lattice, involving a number of vacancies in random distribution, exists therefore in the octahedral layer of stevensite. The formula per half a unit cell is $Mg_x(Mg_{3-x}\square_x)Si_4O_{10}(OH)_2$, $\square$ represents a vacancy. This defect structure explains the low cations exchange capacity of stevensite. After thermal treatment, migration of the magnesium cations can occur, following the so-called Hoffman–Klemen effect.[38] This leads to the transformation of stevensite into talc. Finally, our XRD data indicate that the stevensite/talc ratio decreased in the talc-like phyllosilicate samples when the hydrothermal synthesis temperature increased.

The effect of hydrothermal synthesis temperature was also illustrated on FTIR spectra of Tx phyllosilicates. Fig. 2 (a) and (b) presents the spectra in the 2000–400 and 3800–3600 cm^{-1} frequency ranges, respectively. The infrared spectrum of T160 compound exhibited two bands due to the presence of the physisorbed water, namely the ν(O–H) stretching frequency at 3467 cm^{-1} (not shown) and the δ(O–H) deformation band at 1648 cm^{-1}. It presented also four characteristic vibration bands of natural talc at 3676 cm^{-1} for ν(O–H) in Mg_3OH group, at 1027 cm^{-1} for the overlap of $\nu(Si–O)_{as}$ and ν(Si–O–Si), at 673 cm^{-1} for the overlap of $\nu(Si–O)_s$ and δ(O–H), and at 472 cm^{-1} for the overlap of δ(Si–O–Si) and *trans* (OH) // (translatory vibration of hydroxyl groups, out of phase with the other oxygen atoms in the sheet).[11]

The expected vibration band at 535 cm^{-1} for the Mg–OH ⊥ group (octahedral oxygen atoms and hydroxyl groups, vibrations of octahedra moving in opposition to coordinated Mg^{2+}) appeared only as a small shoulder of the 472 cm^{-1} band. When the hydrothermal synthesis temperature increased the intensity of characteristic bands of physisorbed water decreased and the shape of the other bands changed. The bands at 1027 and 673 cm^{-1} observed for T160 were shifted to 1024 and 669 cm^{-1} for T350, respectively; the first one became broader with the appearance of a shoulder

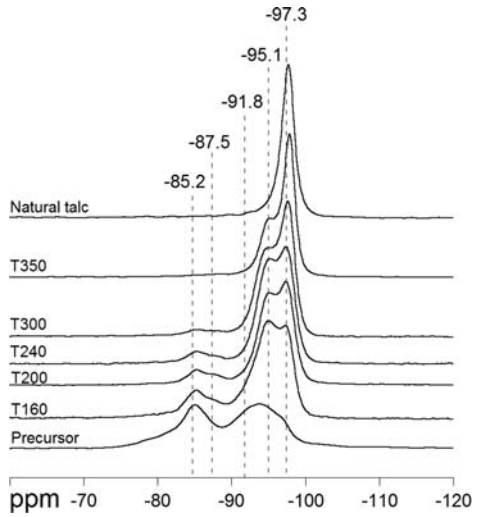

Fig. 3 ^{29}Si CP MAS NMR spectra of precursor, Tx talc-like phyllosilicates and natural talc.

(consequence of the lesser overlapping of ν(Si–O)$_{as}$ and ν(Si–O–Si) bands) and the second one became higher. In T350 spectrum the vibration at 538 cm^{-1} for the Mg–OH $\perp$ group appeared clearly as well as both vibrations δ(Si–O–Si) and *trans* (OH) // at 467 and 449 cm^{-1}, respectively. The effect of these changes was that the T350 spectrum, in 1400–400 cm^{-1} region, was similar to that of the natural talc. Fig. 2 (b) presents the enlargement spectra in the 3800–3600 cm^{-1} region of the natural talc, talc-like phyllosilicates and the precursor dried at 110 °C for 24 h; the precursor spectrum was characterized by a broad band around 3690 cm^{-1} and all Tx spectra exhibited a band at 3676 cm^{-1} with a shoulder at 3687 cm^{-1} which decreased when the hydrothermal synthesis temperature increased. This observation as well as the changes observed for the vibration of Mg–OH $\perp$ group showed that the temperature had a significant effect on the environment of the Mg–OH group; according to the X-ray diffraction results which suggest the presence of stevensite we attributed the 3687 cm^{-1} band to a ν(O–H) in Mg$_2$□OH group (two divalent cations and a vacancy in an octahedral site).

^{29}Si CP MAS NMR spectra of the precursor, talc-like phyllosilicates and natural talc are reported in Fig. 3.

The different types of silicon atoms were named according to the conventional Q^n notation where Q means that the Si atom is bonded to four oxygen atoms and n corresponds to the number of Si–O–Si siloxane bonds. It was demonstrated that the ^{29}Si chemical shift in solid silicates is strongly influenced by the chemical environment of the silicon nucleus and is highly correlated with the degree of SiO_4 tetrahedra polymerization.[39] In the tetrahedral sheets of the 2 : 1 phyllosilicates, tetrahedral Si–O units are in a Q^3 environment and considering the natural talc, the corresponding peak appears at −97.3 ppm.[13] The spectra of all Tx phyllosilicates exhibited between two and five signals at −97.3, −95.1, −91.8, −87.5 and −85.2 ppm which correspond to Q^3 environment for the first two and Q^2 environment for the last three.[29] The presence of the resonance at −97.3 ppm, whatever the sample, showed clearly that the synthesized talc-like phyllosilicates had units with the silicon environment of the talc (Si*(OSi)$_3$(OMg)). Recently, it has been reported that a peak at −95.1 ppm is characteristic of the stevensite mineral,[40] which is expected according to our XRD and FTIR results. Consequently, this resonance was assigned to a silicon nucleus bonded to three OSi groups and one O-lacuna group resulting from the Mg^{2+} vacancy in an octahedral site (Si*(OSi)$_3$(O□)). The peak at −91.8 ppm could correspond to Q^2 units (Si*(OSi)$_2$(OH)$_2$) which contain two hydroxyl groups.[41] Indeed this resonance was mainly detected for T160 which also contains, according to XRD, a significant amount of the precursor phase. According to Borsacchi *et al.*[42] both resonances at −85.2 and −87.5 ppm were assigned to Q^2 units such as silanol present on platelet edges (Si*(OSi)$_2$(OMg)(OH)) or inter-platelets surface silanol or silanol bonded to incompletely coordinated lattice oxygen anions Si*(OSi)$_2$(O□)(OH). This latter was likely in small amounts when the stevensite phase is detected evidencing the presence of octahedral vacancies. Moreover this assignment is in agreement with our ^{1}H MAS NMR spectra (data not shown) that evidence the presence of silanols in the 1.6–2.2 ppm range for the T160 sample. Decomposition of the ^{29}Si MAS NMR spectra recorded under quantitative conditions (spectra not shown) indicated that the resonances corresponding to Q^2 units accounts for 21% of the ^{29}Si signal for T160 and was decreasing when the temperature was raised. The T350 sample did not present Q^2 signals, indicating the total transformation of precursor.

According to the results obtained by X-ray diffraction, FTIR and ^{29}Si MAS NMR spectroscopies, it can be concluded that the synthesized Tx talc-like phyllosilicates presented flaws in their structure. The main defects consist of magnesium lacunas in octahedral sites compensated by Na^+ or Mg^{2+} cations in interlamellar space to counterbalance the loss of positive charge in the sheets. This is supported by the chemical analysis of the samples that leads to the general formula of $Na_{0.2}Mg_{2.9}Si_4O_{10}(OH)_2$ for T160 and T350 samples. This phenomenon was attributed to stevensite-talc interstratified product present in the Tx samples. In the case of sample T160, a treatment with an aqueous solution of strontium chloride led to a decreasing of the sodium amount (from 1.75% wt to 0.12% wt) and the fixation of 1.58% wt of strontium. The remaining sodium was attributed to the precursor whereas the presence of strontium in the interlayer space confirmed the existence of small amount of vacancies in the octahedral sheet. This result is in agreement with former ones indicating that the lower the synthesis temperature, the higher the number of defects is. Indeed, the rising of hydrothermal synthesis temperature from 160 °C to 350 °C increased the proportion of the resonance characteristic of talc from 21% to 61% of the total signal, respectively at the expense of the stevensite phase and the precursor. Chemical analysis after strontium exchange was not accurate enough to estimate with confidence the amount of vacancies in the case of T350 sample.

T160, T240 and T350 materials were characterized by nitrogen adsorption/desorption measurements. The isotherms (not shown) belong to type IV according to the IUPAC classification.[43] The T160 sample presented a significant contribution of microporosity and exhibited a type H2 hysteresis loop characteristic of a mesoporous structure. The contribution from macropores is minor. The T240 and T350 samples presented a type H3 hysteresis loop corresponding to typical clay hysteresis previously attributed to aggregates of plate-like particles leading to slit-shaped pores.[17] The specific surface areas were calculated from nitrogen adsorption isotherms by applying the BET equation.[44] They were influenced substantially by hydrothermal synthesis temperature indeed the values were 544, 270 and 126 m^2 g^{-1} for T160, T240 and T350, respectively.

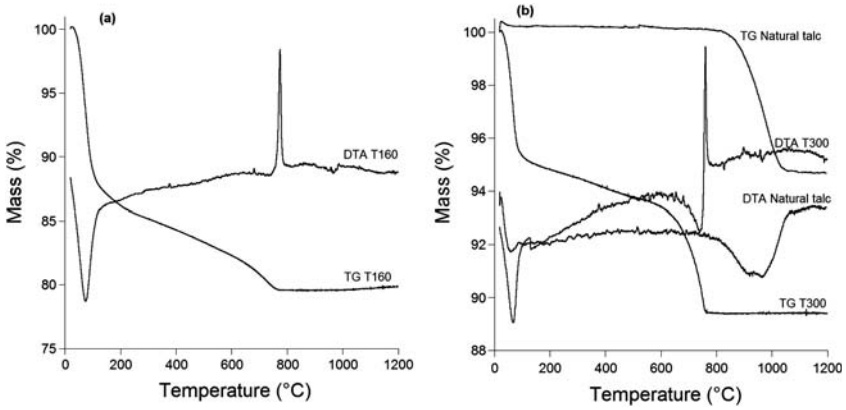

Fig. 4 Thermogravimetric curves of T160 **(a)**, T300 talc-like phyllosilicates and natural talc **(b)**.

The thermal behaviour of the talc-like phyllosilicates and natural talc was investigated by thermogravimetric and differential thermal analyses from 20 to 1200 °C. As example, Fig. 4 (a) presents the corresponding curves for T160; the curves of T300 and natural talc are compared in Fig. 4 (b). Except T160, all Tx talc-like phyllosilicates showed similar thermal continuous degradation with four different mass losses. They appeared on thermogravimetric curves, between 20–140 °C, 140–560 °C, 560–760 and at 760–810 °C; both first and third ones corresponded to endothermic peaks in differential thermal curves whereas the second and fourth ones were exothermic peaks, the T160 sample did not present the third peak.

The first stage was due to the loss of physisorbed water which is characterized in the DTA curve by a peak occurring near 75 °C, whereas the second step corresponds to the loss of interlayer water and the dehydroxylation of the precursor that condensed on heating to yield siloxane bonds. The third loss, corresponding to the endothermic peak at 750 °C, was assigned to the dehydroxylation of the phyllosilicate sheets. This step was followed by the collapse of the sheet structure resulting in the formation of amorphous silica and the crystallisation of enstatite ($MgSiO_3$) which gave the exothermic peak at 770 °C. In order to compare the thermal stability of the T300 sample with that of natural talc we present the thermogravimetric curves in Fig. 4 (b). Due to its hydrophobicity, natural talc did not show mass loss before 735 °C; mass loss was observed, however, from 800 to 1050 °C, corresponding to an endothermic peak at 942 °C observed in differential thermal analysis and assigned to the dehydroxylation of the talc sheets accompanied by the formation of enstatite and silica.[45] For the natural talc these two phenomena are simultaneous while for the synthesized talc-like phyllosilicates the crystallisation of enstatite and the formation of silica followed the dehydroxylation. The lower temperature value (770 °C) observed for decomposition of Tx compounds indicated the lower thermal stability of the talc-like phyllosilicates by comparison with natural talc. The values of the first and second mass losses decreased when the hydrothermal synthesis temperature increased. The first loss was 13.4 and 2.1% for T160 and T350, respectively. These results indicated that the synthesis temperature can control the quantity of physisorbed water in the Tx talc-like phyllosilicates. The second loss was 4.9 and 0.8% for T160 and T350, respectively. The third and fourth mass losses were calculated together, the resulting value was 2.4 and 4.5% for T160 and T350, respectively; it increased when the hydrothermal synthesis temperature increased indicating the decrease of the precursor quantity for the benefit of a well-organized phase. These observations are in agreement with the ^{29}Si NMR data which showed that the hydrothermal synthesis temperature controlled the ratio between the quantities of the precursor residue and crystalline talc-like phyllosilicate together with the number of vacancies in the octahedral sheet.

3.2. Heat treatment and TTx talc-like phyllosilicates characterization

Our objective was the functionalization by covalent grafting of talc-like phyllosilicates; first we synthesized a range of talc-like phyllosilicates with various degrees of hydration to verify that the rate of hydration drives the ability of talc-like phyllosilicates to react and therefore influences the amount of the grafted molecule. The results obtained by X-ray diffraction, infrared and solid-state ^{29}Si NMR spectroscopies and thermogravimetric analyses showed that the lower the hydrothermal synthesis temperature, the higher the rate of hydration and amount of flaws were, the hydration being connected to the lack of magnesium in octahedral sites and the presence of cations in interlamellar space. In order to obtain a good compromise between the quantity of flaws and the ability to react, we chose to carry out a heat treatment of Tx samples rather than to increase the hydrothermal synthesis temperature (>350 °C) or to act on the duration of the synthesis. Thermal treatment of Tx talc-like phyllosilicates consisted of heating for 4 h at 550 °C and led to TTx products.

The X-ray powder diffraction patterns indicated the same peak evolution between the Tx and the corresponding TTx for all hydrothermal synthesis temperatures. The diffraction peaks of TTx samples were more sharp than their Tx counterparts. The (00l) series for TT350 confirmed a sheet structure of the material and indicated the increase of the crystalline coherence along the z axis (Fig. 5 (a)). The (001) diffraction peak underwent an evolution more significant than the other peaks, indeed its shape became more symmetric and the intensity of the small peak at a lower diffraction angle went down. The comparison between the X-ray diffractograms of the TT350 and the natural talc showed that the talc-like phyllosilicate structure was less

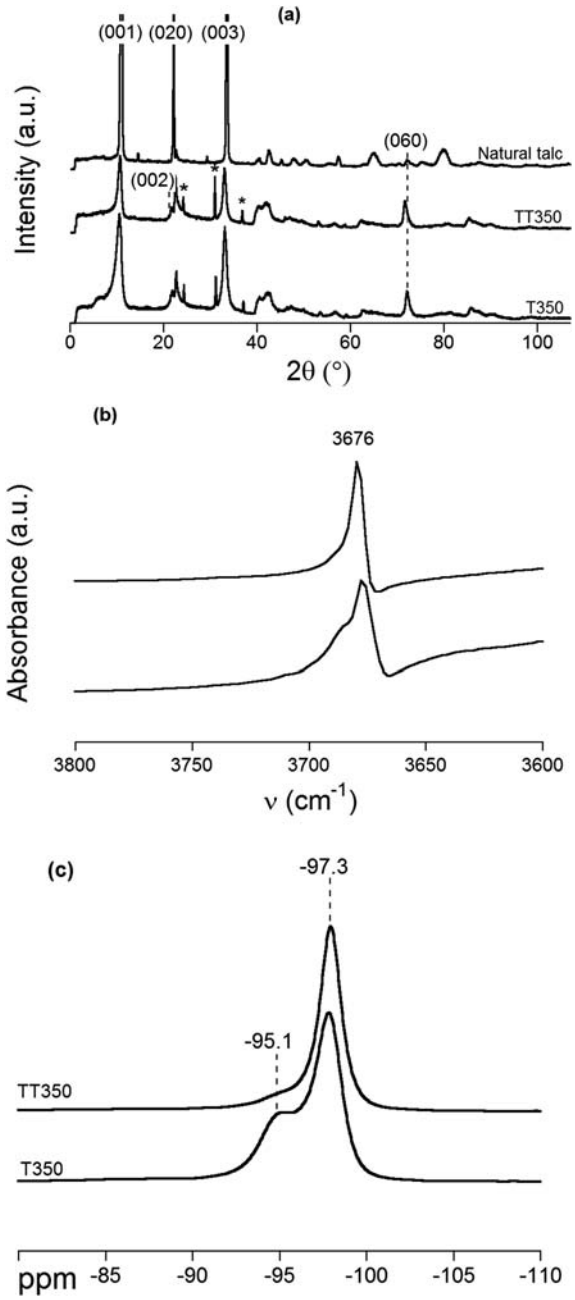

Fig. 5 X-Ray powder diffraction patterns of T350, heat treated TT350 talc-like phyllosilicates and natural talc (* NaCl) **(a)**, enlargement FTIR spectra of heat treated TT350 and T350 talc-like phyllosilicates **(b)**, ^{29}Si CP MAS NMR spectra of T350 and heat treated TT350 talc-like phyllosilicates **(c)**; a.u.: arbitrary unit.

well-organized but the heat treatment led to a structure close to natural talc. The differences between the diffractograms were in the peak intensities (bigger for the natural talc), the full width at half height (bigger for the TT350) and in the position of the (001) peak, (0.941 nm and 0.934 nm for TT350 and the natural talc, respectively; the difference in values is conclusive because the deviation is estimated to 0.004 nm). These observations must be connected to the TEM micrographs which indicated that the particles sizes of Tx and TTx (in the 200–300 nm range) were smaller than those of natural talc (micrometre range). The bigger size of particles led to the well-ordered three-dimensional structure for the natural talc and therefore an increase of the intensity of the diffraction peaks compared with the synthetic talc-like phyllosilicates.

The TTx talc-like phyllosilicates presented similar FTIR spectra to their corresponding Tx except for the shoulder at 3687 cm^{-1} attributed to ν(O–H) vibration in $Mg_2\square OH$. After heat treatment, the shoulder intensity decreased in TTx (x = 160, 200, 240 and 300) spectra and it disappeared in the TT350 spectrum (Fig. 5 (b)). The ^{29}Si CP MAS NMR analyses indicated clearly the effect of the heat treatment on the structure of the talc-like phyllosilicates. Indeed the intensity of peaks at −85.2, −87.5, −91.8 and −95.1 ppm, that are not characteristic of talc, decreased for all TTx samples comparatively to their counterpart Tx; the TT350 talc-like phyllosilicate exhibited a main peak at −97.3 ppm with a small one at −95.1 ppm accounting for only 4% of the total signal (Fig. 5 (c)). The decomposition of the spectra recorded in quantitative conditions allows the determination of the proportion of each resonance. Taking into account only the area of the signals at −97.3 ppm (characteristic of talc) and −95.1 ppm (assigned to stevensite), it is possible (after normalisation to 1) to derive a talc/stevensite ratio of 0.27, 0.56, 0.67 and 0.96 for the samples T160, TT160, T350 and TT350, respectively. Consequently by adjusting the hydrothermal synthesis temperature or by performing an additional annealing at 550 °C, a fine tuning of the defects level in the talc-like phyllosilicate structure is feasible.

TT160, TT240 and TT350 materials were characterized by nitrogen adsorption/desorption measurements. They presented the same type IV and H hysteresis loop as the parent samples but the heat treatment suppressed the mesoporous structure for TT160 and increased the macroporous structure for all samples; this increase was attributed to a growth of particles during the annealing. Heat treatment produced a strong decrease of specific surface areas, from 544 to 321 $m^2\ g^{-1}$ for T160 and TT160, respectively, from 270 to 188 $m^2\ g^{-1}$ for T240 and TT240,

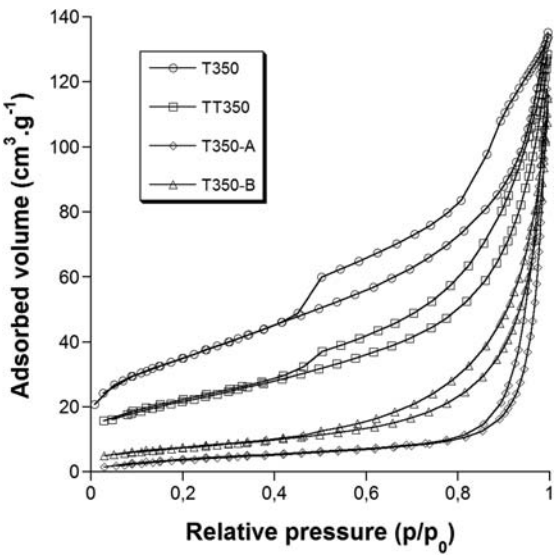

Fig. 6 Nitrogen adsorption/desorption isotherms for T350, TT350, T350-A and T350-B.

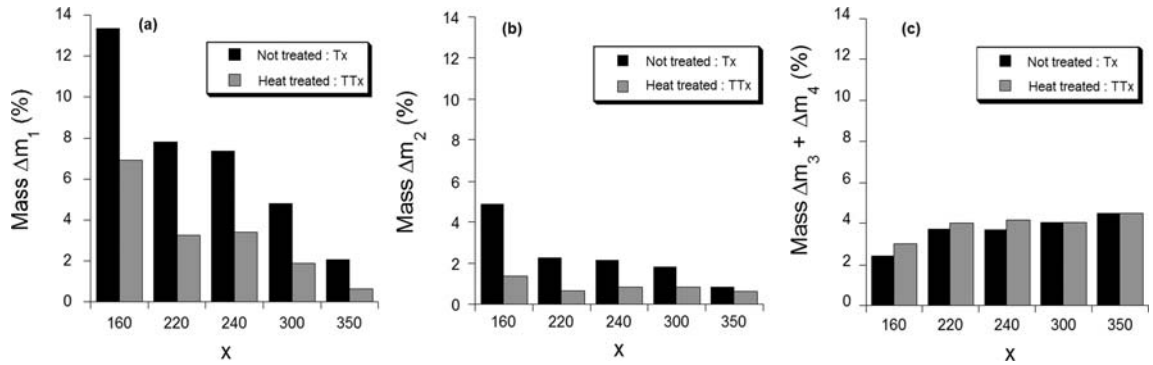

Fig. 7 Evolution of the first mass loss **(a)**, second mass loss **(b)** and third plus fourth mass losses **(c)**, calculated from thermogravimetric data, for the Tx and TTx talc-like phyllosilicates.

respectively, and from 126 to 78 $m^2\ g^{-1}$ for T350 and TT350, respectively. The comparison between the specific surface areas of natural talcs (in the 1.5–6.6 $m^2\ g^{-1}$ range, according to their purity)[46] with those of T350 and TT350 indicated that their surface properties were different enough to consider the quantitative grafting of T350 and TT350. Nitrogen adsorption/desorption isotherms for T350 and TT350 are shown in Fig. 6.

The thermogravimetric and differential thermal curves of TTx showed the four different mass losses observed for the Tx samples. The difference was the values of the first and second losses which decreased after heat treatment, the first losses were 6.9 and 0.6% for TT160 and TT350, respectively, and the second losses were 1.4 and 0.6%, respectively. The resulting values of third and fourth mass losses increased slightly for 160, 200 and 240 °C temperatures but it remained constant for 300 and 350 °C temperatures (Fig. 7).

The different analyses indicated that the thermal treatment allowed a flaw reduction in talc-like phyllosilicate structure and thus the increase of the talc/stevensite ratio. During the thermal treatment, Mg^{2+} cations present in the interlamellar space migrated into the lacunas resulting in the talc structure, the TT350 structure being the closest to that of talc.

Table 1 Nitrogen, carbon and hydrogen mass percentages obtained from the elemental analyses; (ideal values) calculated from nitrogen and carbon percentage for hybrids-A and hybrids-B, respectively. Grafted amounts, τ, expressed in millimoles of organosilane per gram of talc-like phyllosilicate calculated from elemental analysis and thermogravimetric data. Specific surface areas, S, expressed in $m^2\ g^{-1}$

	EA %N	EA %C	EA %H	τ(EA)	τ(TGA)	S
T160-A	4.97 (4.97)	15.50 (17.09)	3.16 (3.20)	1.78	2.05	6
TT160-A	2.69 (2.69)	7.82 (9.22)	1.76 (1.73)	0.96	0.97	—
T160-B		10.67 (10.67)	1.10 (0.98)	0.49	0.63	15
T240-A	4.79 (4.79)	15.76 (16.42)	2.66 (3.08)	1.71	1.70	8
T240-B		9.26 (9.26)	0.96 (0.86)	0.43	0.45	16
T350-A	2.71 (2.71)	8.16 (9.31)	1.65 (1.75)	0.97	0.94	16
TT350-A	0.50 (0.50)	1.99 (1.73)	0.29 (0.32)	0.18	0.24	—
T350-B		5.61 (5.61)	0.64 (0.52)	0.26	0.27	27
Natural talc-A	0.65 (0.65)	2.17 (2.21)	0.43 (0.41)	0.23	0.30	—
Natural talc-B		0.31 (0.31)	0.08 (0.02)	0.01	0.02	—

3.3. Grafted materials

We investigated the grafting reaction of two organotriethoxysilanes (Scheme 1), N-(3-triethoxysilylpropyl)-4,5-dihydroimidazole (IM2H) and 2-hydroxy-4-(3-triethoxysilylpropoxy)-diphenylketone (HTDK), on Tx samples in order to demonstrate that the synthetic talc-like phyllosilicates can be chemically functionalized with different grafted amounts under mild conditions. The physico-chemical properties of synthetic Tx evolved gradually with the synthesis temperature, and we explored the grafting reaction on three Tx samples (x = 160, 240 and 350) representative of the evolution of properties. To evaluate the effect of thermal treatment on the reactivity of synthetic talc-like phyllosilicates we also realized the grafting reaction on TTx (x = 160, 240 and 350) with IM2H. The reactions were carried out by stirring for 48 h at 110 °C a mixture of the organoalkoxysilane and the talc-like phyllosilicate in toluene solvent. The obtained hybrids are designated Tx-A (or TTx-A) and Tx-B when IM2H and HTDK were used, respectively.

The grafted amounts, τ, expressed in millimoles of organosilane per gram of talc-like phyllosilicate are gathered in Table 1; they were computed from the nitrogen or carbon content obtained by elemental analysis and they were confirmed by thermogravimetric data. According to the hypothesis that the chemical grafting happens on the surface hydroxyl groups, the grafted amount should be dependent on the hydrothermal synthesis temperature; this was observed since for both organoalkoxysilanes the grafted amounts became smaller when the hydrothermal synthesis temperature increased. However IM2H and HTDK presented different behaviour toward the grafting reaction, indeed for each Tx the amount of grafted organic groups was higher when IM2H was used (in the range 1.78–0.97 mmol g^{-1}) and HTDK gave rates approximately three times lower (in the range 0.49–0.26 mmol g^{-1}). The grafted amount variations must not be interpreted only by surface hydroxyl groups but also by the great influence of physisorbed water on the Tx or TTx materials. Indeed, in the grafting process concurrent reactions can be observed as hydrolysis of alkoxysilane functions, condensation of hydrolyzed species on material surface, but also oligomerization from hydrolyzed species, condensation of oligomers on material surface and anarchical polymerization on material surface. The two last reactions lead to a vertical multilayer polymerization which can be prevented by balancing the hydrolysis reactions

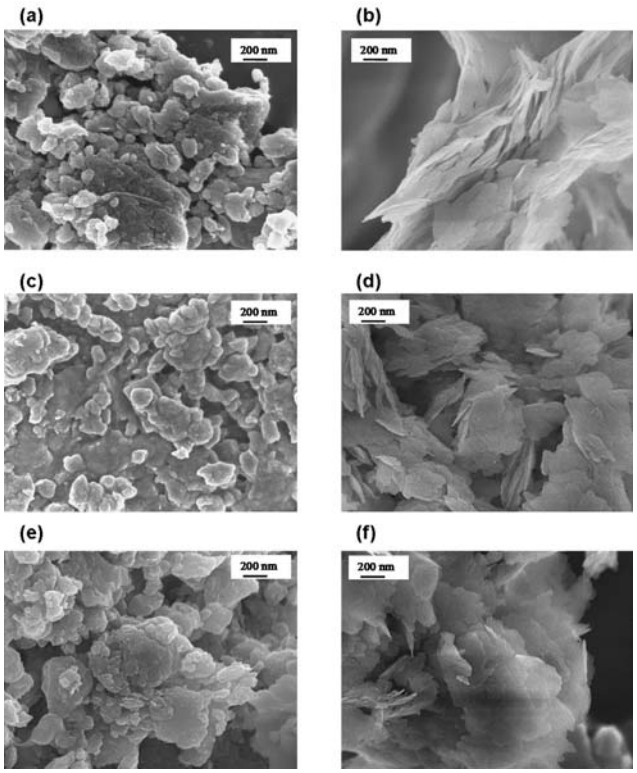

Fig. 8 SEM micrographs for T160 **(a)**, T350 **(b)** talc-like phyllosilicates; T160-A **(c)**, T350-A **(d)**, T160-B **(e)** and T350-B **(f)** hybrids.

and the condensation reactions.[47–50] The variation of grafted amount of IM2H and HTDK with the hydrothermal synthesis temperature, and therefore with physisorbed water amount, suggests that an excess of water provokes an anarchical and vertical polymerization as observed with the MCM-41 functionalization.[49] The higher grafted amount found with IM2H suggests the easier polymerisation of IM2H alkoxyl functions compared to HTDK ones.

In order to compare the synthetic phyllosilicate's ability to react with that of the talc we also grafted the natural talc. It resulted that the smallest rates (0.97 and 0.26 mmol g^{-1} for IM2H and HTDK, respectively) observed for T350 were bigger than those found with the natural talc (0.23 and 0.01 mmol g^{-1} for IM2H and HTDK, respectively). The thermal treatment of talc like phyllosilicates led to a substantial decrease of grafted amounts, indeed the values were 0.97 and 0.18 mmol g^{-1} for T350-A and TT350-A, respectively. The small difference between the grafted amounts of TT350-A and natural talc (0.18 and 0.23 mmol g^{-1}) must be connected with physico-chemical characterizations which indicated that the TT350 structure was very close to that of natural talc. The SEM micrographs indicated that the grafting did not affect the morphology of talc-like phyllosilicates when the grafting amount was low (<1 mmol g^{-1}); indeed the surface of hybrids T160-B, T350-A and T350-B looked like the surface of parent Tx whereas in the T160-A sample the particles seemed slightly more connected (Fig. 8). It is also worthy to note the linear correlation between the grafted amounts of IM2H and the talc/stevensite ratio derived from ^{29}Si MAS NMR experiments which underlies the importance of the presence of defaults for a better grafting.

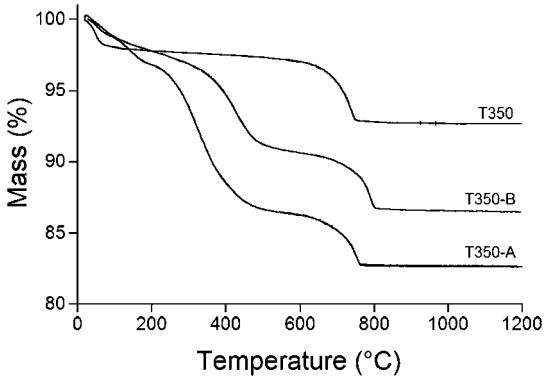

Fig. 9 Thermogravimetric curves of T350-A, T350-B hybrids and T350 talc-like phyllosilicate.

Significant changes in the nitrogen adsorption–desorption isotherms were observed upon grafting talc-like phyllosilicates with IM2H and HTDK, they are illustrated for T350-A and T350-B in Fig. 6. The specific surface areas of hybrids, in the 6–27 $m^2 g^{-1}$ range, are substantially lower that the Tx ones (in the 544–126 $m^2 g^{-1}$ range), this trend was previously observed when laponite clays particles[47] or silica nanoparticles[48] were grafted. According to the hypothesis that organic modification depends on surface hydroxyl groups and physisorbed water quantities, the extent of specific surface areas decrease should be dependent on the hydrothermal synthesis temperature (and therefore on the grafted amount). This was indeed observed since, for both organotriethoxysilanes, the specific surface areas of hybrids was increasingly higher when hydrothermal synthesis temperature was high (6, 8 and 16 $m^2 g^{-1}$ for T160-A, T240-A and T350-A, respectively and 15, 16 and 27 $m^2 g^{-1}$ for T160-B, T240-B and T350-B).

In the thermogravimetric curves, additional weight losses were observed for the hybrid samples compared to the parent Tx or TTx. For example, Fig. 9 presents the thermogravimetric curves for the T350, T350-A and T350-B samples. The losses appeared in differential thermal curves (not shown) as exothermic processes, at 250 and 360 °C for Tx-A and TTx-A, and at 340 and 375 °C for Tx-B. These decompositions were clearly associated with the organic group degradation and suggested that the silanes were strongly bound on the talc-like phyllosilicate.[21] The

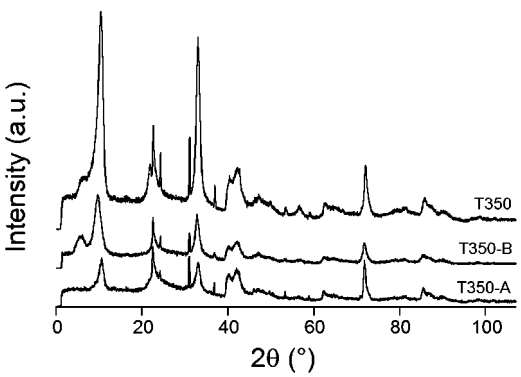

Fig. 10 X-Ray powder diffraction patterns of T350-A, T350-B hybrids and T350 talc-like phyllosilicate; a.u.: arbitrary unit.

grafted amounts were estimated by measuring these weight losses although it was difficult to determine accurately the amount of organics because these losses were partially mixed with losses of interlayer water and precursor dehydroxylation of the talc-like phyllosilicates. Therefore the deviation of grafted amount calculated from thermogravimetric data is higher than that of the values calculated from elemental analysis data; even so we chose to calculate them only to compare the values. We found 2.05, 0.94, 0.63 and 0.27 mmol g^{-1} for T160-A, T350-A, T160B and T350-B, respectively. These values, as indicated in Table 1, are in agreement with those calculated by elemental analysis. The thermogravimetric curves also informed us about the hybrid structure, indeed the exothermic peaks corresponding to the collapse of the sheet structure were observed at 770 °C and 810 °C for Tx-A and Tx-B hybrids, respectively, while the parent Tx gave a peak at 770 °C. The temperature shift observed for the Tx-B hybrids indicated a change in the structure and the bigger stability induced by the grafting of HTDK organosilane.

The X-ray powder diffraction patterns of the T350, T350-A and T350-B samples are shown in Fig. 10. The X-ray powder diffraction patterns of T350-A and T350-B hybrids showed the (001), (020), (003) and (060) characteristic reflections of talc structure but the (002) reflection did not appear. The (001) reflection observed for T350 was considerably affected by the grafting since T350-A did not present the shoulder observed for T350, furthermore T350-B exhibited a peak at lower diffraction angle clearly separated from (001). For T350-A the basal $d_{(001)}$ value (0.944 nm) was slightly higher than that of T350 (0.941 nm), but the difference is not conclusive because the deviation is estimated to 0.004 nm.

This very slight enlargement of the interlayer space indicated that the grafting of IM2H did not lead to intercalation of organic groups. Indeed, if the grafting led to intercalation of organic groups the basal $d_{(001)}$ interlayer separation of the hybrids must be significantly higher in the T350 one (0.941 nm); the 0.944 nm value must be connected with 1.32 nm for the basal $d_{(001)}$ interlayer separation in a talc-like hybrid obtained by the one step sol–gel synthesis from $MgCl_2$ and IM2H in ethanolic solution; in this hybrid the organic groups compulsorily occupy the interlayer spaces but it presents a low crystallinity.[16] The grafting of HTDK did not present similar trends since T350-B presented two peaks in the small angles which corresponded to the basal $d_{(001)}$ interlayer separations of 0.946 and 1.585 nm. The reason for the presence of two peaks is not fully understood at this stage, but the expansion to 1.585 nm in the interlayer distance might be due to the grafting of HTDK in the interlayer spaces. The basal $d_{(001)}$ interlayer expansion must connect with thermogravimetric and grafted amounts data; indeed the structure collapse temperatures for Tx-A and Tx-B hybrids indicated that the grafting produced a change in the Tx-B hybrids structure. On the other hand, the higher grafted amount found with IM2H suggest the easier polymerisation of IM2H comparatively to HTDK; the numerous hydrolyzed HTDK monomers could be grafted in the interlayer spaces whereas the steric hindrance of IM2H oligomers could forbid this grafting type.

The covalent attachment of organic groups to the Tx or TTx talc-like phyllosilicates was evidenced by ^{29}Si CP MAS NMR spectroscopy. The T160, T160-A, T160-B and T350, T350-A, T350-B spectra are shown in Fig. 11 (a) and (b), respectively. The signals of the ungrafted IM2H or HTDK molecules (−45.3 and −46.6 ppm, respectively) have never been observed in any samples indicating the absence of physisorbed organoalkoxysilanes on the talc-like phyllosilicates. The Tx-A hybrids spectra exhibited two new signals at −67.1 and −58.6 ppm which are characteristic of the presence of Si–C bonds in the structure. In agreement with the low grafted amount of HTDK the two peaks were not observed in the Tx-B hybrids spectra although the CP MAS technique was used. The assignments of the resonances were based on previous results for analogous systems which involved modified silica[48] or phyllosilicates.[20,51] The signal at −67.1 ppm was attributed to the Si* atom in $RSi^*(OSi)_3$ unit (T^3) where R represents the pendant organic group. The small peak at −58.6 ppm was assigned to the Si* atom in $RSi^*(OSi)_2(OEt)$ unit (T^2) where one ethoxy function was not hydrolyzed according to the anhydrous grafting conditions.

A complete hydrolysis of organoalkoxysilane was not expected on the basis of the lowest reactivity of alkyltrialkoxysilane and because the condensation reaction always begins before the complete hydrolysis.[29,52] It is interesting to note that relative proportion of grafted species can also be derived from quantitative ^{29}Si MAS NMR measurements (spectra not shown). Indeed the signal corresponding to T^2 and T^3 units account for 21 and 10% of the total signal for T160-A and T350-A, respectively. These data indicate that grafting was twice as successful for T160

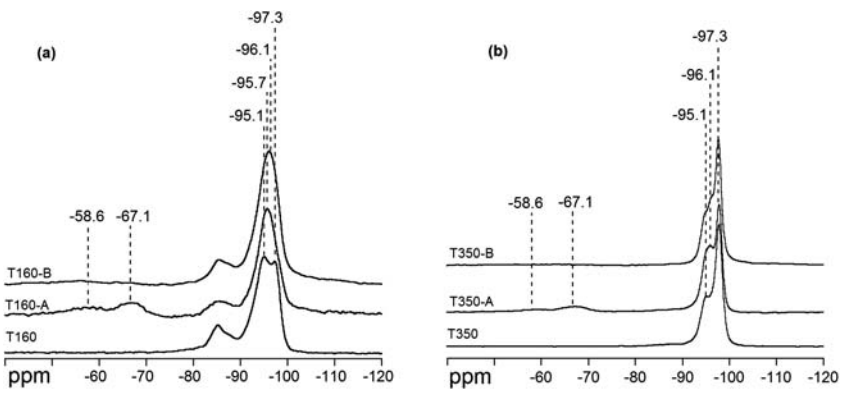

Fig. 11 ^{29}Si CP MAS NMR of T160 talc-like phyllosilicate and T160-A, T160-B hybrids **(a)** and T350 talc-like phyllosilicate and T350-A, T350-B hybrids **(b)**.

than for T350 in agreement with both elemental and thermal analysis (see Table 1). The grafting reaction also produced changes in the Q^3 peaks region since T160-A and T160-B presented one broad signal at −95.7 ppm and −96.1 ppm, respectively, instead of the two observed signals at −97.3 and −95.1 ppm for T160. The T350-A sample presented a relatively broad peak at −95.7 and a sharp peak at −97.3 ppm while T350-B exhibited three signals at −95.1 ppm, −96.1 ppm and −97.3 ppm, the signals at −95.1 and −97.3 ppm being observed in the T350 sample. These observations indicated that the grafting of HTDK on T350 produces changes in the sheet structure as observed in XRD analysis. Previously, we noticed that the hydrothermal synthesis temperature influenced the composition of the Tx talc-like phyllosilicates which differ in the talc/stevensite ratio and the quantity of precursor. The different compositions of Tx led to different hybrids; indeed the grafting reaction on the T160 sample induced the intensity decrease of the peak at −85.2 ppm indicating that the grafting also took place at the Q^2 unit (silanol) whereas this grafting was unable to occur in the T350 sample. This may explain the higher (roughly twice) grafted amount obtained in the case of T160.

FTIR and DRIFT analyses were used as an important tool to confirm the covalent bonding of organosilane. All hybrids of the same type (Tx-A or Tx-B) presented similar absorption spectra, the difference being in the band intensities; indeed when the grafting amount was low the band intensities for the vibration of organic moieties were weak. The characteristic band for the overlap of $\nu(\text{Si–O})_{as}$ and ν(Si–O–Si) observed in the range 1024–1027 cm^{-1} for the Tx or TTx samples was disturbed indicating the grafting on silanol functions as already suggested by solid-state ^{29}Si NMR. Indeed in the hybrid spectra this band underwent a broadening and the appearance of a ν(Si–C) vibration as a shoulder in the range 1197–1212 cm^{-1}. The Tx-A spectra showed an intensity decrease of the ν(O–H) band in the Mg_3OH group, which implies that the alkoxyorganosilanes reacted also with the Mg–OH groups as observed in natural talc.[21] For both grafted organosilanes IM2H and HTDK (developed structures described in Scheme 1), classical methylene stretching vibrations of the propyl chain appeared at 2947–2952 and 2897–2904 cm^{-1} for asymmetric and symmetric ν(C–H), respectively. However the complete integrity of the organic functions grafted on talc-like phyllosilicates can't be confirmed by DRIFT or FTIR spectroscopies; indeed the strong δ(O–H) band of the water can overlap the ν(C=N) vibration expected at 1606 cm^{-1} for IM2H or the ν(C=O) vibration expected at 1624 cm^{-1} for HTDK. In the Tx-A spectra the presence of an unexpected band at 1570 cm^{-1} suggested the appearance of amide function and therefore the hydrolysis of the 4,5-dihydroimidazole ring.

^{13}C CP MAS NMR spectroscopy is an important tool to elucidate the structure of the silylating agents grafted on the talc-like phyllosilicates. All Tx-A and Tx-B spectra showed two resonances in the range 17.9–18.3 ppm and 58.9–57.6 ppm associated with the methyl and methylene groups, respectively, of the ethoxy functions in the alkoxyorganosilane. This result was in agreement with the ^{29}Si CP MAS NMR spectroscopy which indicated incomplete hydrolysis of the alkyltrialkoxysilane functions. For Tx-B samples the integrity of the organic group was confirmed and the full assignment according to the carbon atom indexation is illustrated in Scheme 1.[53] On the other hand in the Tx-A spectra the resonance at 157.8 ppm of the carbon atom in the –N=CHN– group has never been observed but a signal characteristic of HOCNH– amide group appeared at 165.1 ppm. The resonances at 55.0 and 48.2 ppm of methylene groups in the 4,5-dihydroimidazole ring were shifted to 48.8 ppm and 39.9 ppm (C_2 and C_3) for the grafted Tx-A.[53] The signals of the methylene groups in the linear chain didn't undergo significant shift. These results are in agreement with the hydrolysis of 4,5-dihydroimidazole ring and therefore its opening (Scheme 2) during the grafting process as suggested by the DRIFT analysis.

The behaviour of the IM2H molecule was probably due to intramolecular interactions between the hydrolyzed triethoxysilyl group and the 4,5-dihydroimidazole ring.[54] The hydrolysis of –N=CHN– group ending in the linear amide molecule could explain the better grafted amounts found for Tx-A hybrids. Indeed the linear amide presents more flexibility and less steric hindrance than the rigid dicyclic HTDK and the consequence was a higher grafting amount.

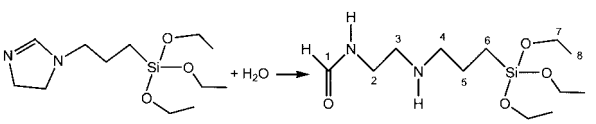

Scheme 2 Hydrolysis reaction of 4,5-dihydroimidazole ring.

4. Conclusion

A range of talc-like phyllosilicates were prepared *via* a hydrothermal synthesis performed at five different temperatures (160, 200, 240, 300 and 350 °C). Transmission electronic microscopy indicated that the particles size of talc-like phyllosilicates was in the nanometre range. The different analyses indicated that the temperature of hydrothermal synthesis strongly influenced the crystallinity and the composition of materials. When the synthesis temperature was low the material presented high degree of hydration, low crystallinity and flawed structure. The defects consisted of magnesium lacunas in octahedral sites which were compensated by Na^+ or Mg^{2+} cations in interlamellar space to counterbalance the loss of positive charge in the sheets. This was attributed to stevensite-talc interstratified product present in the samples. The ratio stevensite/talc and the hydration decreased in the talc-like phyllosilicate samples when the hydrothermal synthesis temperature increased and the crystallinity became higher. A thermal treatment at 500 °C allowed a significant flaw reduction in talc-like phyllosilicate structure and a sample synthesized at 350 °C and heat treated presented a structure close to that of talc. The different talc-like phyllosilicates were grafted covalently by two organoalkoxysilane reagents. The condensation reaction involved hydroxyl groups on talc-like phyllosilicates and the triethoxysilyl functions of organic reagents. The grafted amounts of the hybrids were dependent on the hydrothermal synthesis temperature and organoalkoxysilanes; they became smaller when the synthesis temperature increased and when HTDK was used. For IM2H the grafting did not modify the original inorganic structure of the support but for HTDK it seems that the grafting took place in the interlayer spaces. During the grafting process the –N=CHN– group of cyclic IM2H was

hydrolyzed ending in a linear amide group which presents more flexibility and less steric hindrance than the rigid dicyclic HTDK. The new hybrids may be promising in lubricant coatings so now investigations into their tribological properties are in progress.

References

1 J. Livage, T. Coradin and C. Roux, in *Functional Hybrid Materials*, ed. P. Gomez Romero and C. Sanchez, Wiley-VCH, Weinheim, 2004.
2 C. Sanchez, B. Julián, P. Belleville and M. Popall, *J. Mater. Chem.*, 2005, **15**, 3559–3592.
3 F. Martin, J.-P. Bonino, P. Bacchin, P. Vaillant, E. Ferrage, W. Vautrin, Ph. Barthes, WO2004/063428, PCT/FR2003/03625.
4 F. Martin, J.-P. Bonino, P. Micoud, J. Ferret, C. Lebre, V. Baylac, Fr. Pat., FR 2007/08875, PCT/FR2008/052351.
5 J. H. Rayner and G. Brown, *Clays Clay Miner.*, 1973, **21**, 103–114.
6 R. F. Giese, *Clays Clay Miner.*, 1979, **27**, 213–223.
7 B. Perdikatsis and H. Burzlaff, *Z. Kristallogr.*, 1981, **156**, 177–186.
8 W. F. Bleam, *Clays Clay Miner.*, 1990, **38**, 522–526.
9 K. E. Bremmell and J. Addai-Mensah, *J. Colloid Interface Sci.*, 2005, **283**, 385–391.
10 J. J. Hemley, J. W. Montoya, C. L. Christ and P. B. Hostetler, *Am. J. Sci.*, 1977, **277**, 322–351.
11 F. Martin, P. Micoud, L. Delmotte, C. Marichal, R. Le Dred, P. de Parseval, A. Mari, J.-P. Fortuné, S. Salvi, D. Béziat, O. Grauby and J. Ferret, *Can. Mineral.*, 1999, **37**, 997–1006.
12 S. Petit, F. Martin, A. Wiewiora, P. de Parseval and A. Decarreau, *Am. Mineral.*, 2004, **89**, 319–326.
13 F. Martin, E. Ferrage, S. Petit, P. de Parseval, L. Delmotte, J. Ferret, D. Arseguel and S. Salvi, *Eur. J. Mineral.*, 2006, **18**, 641–651.
14 A. L. de Faria, C. Airoldi, F. G. Doro, M. G. Fonseca and M. D. Assis, *Appl. Catal., A*, 2004, **268**, 217–226.
15 Y. Fukushima and M. Tani, *J. Chem. Soc., Chem. Commun.*, 1995, 241–242.
16 N. T. Whilton, S. L. Burkett and S. Mann, *J. Mater. Chem.*, 1998, **8**, 1927–1932.
17 K. A. Carrado, L. Xu, R. Csencsits and J. V. Muntean, *Chem. Mater.*, 2001, **13**, 3766–3773.
18 C. R. Silva, M. G. Fonseca, J. S. Barone and C. Airoldi, *Chem. Mater.*, 2002, **14**, 175–179.
19 J. A. A. Sales, G. C. Petrucelli, F. J. V. E. Oliveira and C. Airoldi, *J. Colloid Interface Sci.*, 2006, **297**, 95–103.
20 J.-C. Gallégo, M. Jaber, J. Miehé-Brendlé and C. Marichal, *New J. Chem.*, 2008, **32**, 407–412.
21 M. G. da Fonseca and C. Airoldi, *Mater. Res. Bull.*, 2001, **36**, 277–287.
22 J. M. Raquez, Y. Nabar, R. Narayan and P. Dubois, *Macromol. Mater. Eng.*, 2008, **293**, 310–320.
23 J. F. Alcover and R. F. Giese, *Clay Miner.*, 1986, **21**, 159–169.
24 F. Martin, J. Ferret, C. Lebre, S. Petit, O. Grauby, J.-P. Bonino, D. Arseguel, A. Decarreau, C. Ferrage, Fr. Pat. FR 2006/06473, PCT/FR 2007/001200.
25 F. Martin, J. Ferret, C. Lebre, S. Petit, O. Grauby, J.-P. Bonino, D. Arseguel, A. Decarreau, C. Ferrage, Fr. Pat. FR 2006/06474, PCT/FR 2007/001201.
26 F. Martin, J. Ferret, C. Lebre, S. Petit, O. Grauby, J.-P. Bonino, D. Arseguel, A. Decarreau, C. Ferrage, Fr. Pat. FR 2006/06476, PCT/FR 2007/001202.
27 A. Decarreau, H. Mondesir and G. Besson, *C.R. Acad. Sci., Ser. IIc: Chim.*, 1989, **308**, 301–306.
28 E. F. Vansant, P. Van der Voort, K. C. Vranckren, in *Characterisation and Chemical Modification of the Silica Surface*, ed. B. Delmon and J. T. Yates, Elsevier, Amsterdam, 1st edn, 1995.
29 C. J. Brinker and G. W. Scherer, in *Sol–Gel Science, The Physics and Chemistry of Sol–Gel Processing*, ed. Academic Press, San Diego, 1990.
30 D. Massiot, F. Fayon, M. Capron, I. King, S. LeCalvé, B. Alonso, J.-O. Durand, B. Bujol, Z. Gan and G. Hoatson, *Magn. Reson. Chem.*, 2002, **40**, 70–76.
31 I. S. Stemple and G. W. Brindley, *J. Am. Ceram. Soc.*, 1960, **43**, 34–42.
32 E. Ferrage, G. Seine, A.-C. Gaillot, S. Petit, P. De Parseval, A. Boudet, B. Lanson, J. Ferret and F. Martin, *Eur. J. Mineral.*, 2006, **18**, 483–491.
33 S. L. Burkett, A. Press and S. Mann, *Chem. Mater.*, 1997, **9**, 1071–1073.
34 D. D. Eberl, B. F. Jones and H. N. Khoury, *Clays Clay Miner.*, 1982, **30**, 321–326.
35 M. Jaber, J. Miéhé-Brendlé, L. Delmotte and R. Le Dred, *Solid State Sci.*, 2005, **7**, 610–615.
36 JCPDS Card Number 13–0558.
37 G. T. Faust, J. C. Hathaway and G. Millot, *Am. Mineral.*, 1959, **44**, 342–370.
38 U. Hoffman and R. Klemen, *Z. Anorg. Chem.*, 1950, **262**, 95–99.
39 E. Lippmaa, M. Mägi, A. Samoson, M. Tarmac and G. Engelhardt, *J. Am. Chem. Soc.*, 1980, **102**, 4889–4893.
40 B. Rhouta, H. Kaddami, J. Elbarqy, M. Amjoud, L. Daoudi, F. Maury, F. Senocq, A. Maazouz and J.-F. Gerard, *Clay Miner.*, 2008, **43**, 393–403.
41 G. Engelhardt, D. Michel, in *High resolution solid state NMR of silicates and zeolites*, John Wiley & sons, Chichester, 1987.
42 S. Borsacchi, M. Geppi, L. Ricci, G. Ruggeri and C. A. Veracini, *Langmuir*, 2007, **23**, 3953–3960.
43 K. S. W. Sing, D. H. Everett, R. A. W. Haul, L. Moscou, R. A. Pierotti, J. Rouquerol and T. Siemieniewska, *Pure Appl. Chem.*, 1985, **57**, 603–619.
44 S. Brunauer, P. Hemmett and E. Teller, *J. Am. Ceram. Soc.*, 1938, **60**, 309–319.
45 L. A. Pérez-Maqueda, V. Balek, J. Poyato, J. Subrt, M. Benes, V. Ramirez-Valle, I. M. Buntseva, I. N. Beckman and J. L. Pérez-Rodriguez, *J. Therm. Anal. Calorim.*, 2008, **92**, 253–258.
46 C. Nkoumbou, F. Villieras, D. Njopwouo, C. Y. Ngoune, O. Barres, M. Pelletier, A. Razafitianamaharavo and J. Yvon, *Appl. Clay Sci.*, 2008, **41**, 113–132.
47 N. N. Herrera, J.-M. Letoffe, J.-P. Reymond and E. Bourgeat-Lami, *J. Mater. Chem.*, 2005, **15**, 863–871.
48 S. Cousinié, M. Gressier, P. Alphonse and M.-J. Menu, *Chem. Mater.*, 2007, **19**, 6492–6503.
49 T. Martin, A. Galarneau, D. Brunel, V. Izard, V. Hulea, A. C. Blanc, S. Abramson, F. Di Renzo and F. Fajula, *Stud. Surf. Sci. Catal.*, 2001, **135**, 4849–4856.
50 D. Brunel, A. C. Blanc, A. Galarneau and F. Fajula, *Catal. Today*, 2002, **73**, 139–152.
51 M. A. Melo Jr., F. J. V. E. Oliveira and C. Airoldi, *Appl. Clay Sci.*, 2008, **42**, 130–136.
52 R. K. Iler, in *The chemistry of silica*, Wiley, New York, 1979.
53 ^{13}C CP MAS NMR assignments (δ ppm): Tx-A: 165.1 (C1), 57.6 (C7), 48.8 (C3 and C4), 39.9 (C2), 22.8 (C5), 18.3 (C8), 8.7 (C6). Tx-B: 200.1 (C7), 165.9 (C2′ and C4′), 136.6 (C1 and C6′), 128.4 (C2, C3, C4, C5 and C6), 112.4 (C1′), 107.7 (C5′), 104.2 (C3′), 69.8 (C8), 58.9 (C11), 22.2 (C9), 17.9 (C12), 7.8 (C10).
54 J. C. Saam and H. M. Bank, *J. Org. Chem.*, 1965, **30**, 3350–3354.